



Superconductivity in metastable phases of phosphorus-hydride compounds under high pressure

José A. Flores-Livas,¹ Maximilian Amsler,² Christoph Heil,³ Antonio Sanna,⁴ Lilia Boeri,³ Gianni Profeta,⁵ Chris Wolverton,² Stefan Goedecker,¹ and E. K. U. Gross⁴

¹*Department of Physics, Universität Basel, Klingelbergstr. 82, 4056 Basel, Switzerland*

²*Department of Materials Science and Engineering, Northwestern University, Evanston, Illinois 60208, United States*

³*Institute of Theoretical and Computational Physics, Graz University of Technology, NAWI Graz, 8010 Graz, Austria*

⁴*Max-Planck Institut für Mikrostruktur Physics, Weinberg 2, 06120 Halle, Germany*

⁵*Dipartimento di Fisica Università degli Studi di L'Aquila and SPIN-CNR, I-67100 L'Aquila, Italy*

(Received 7 December 2015; published 26 January 2016)

Hydrogen-rich compounds have been extensively studied both theoretically and experimentally in the quest for novel high-temperature superconductors. Reports on sulfur hydride attaining metallicity under pressure and exhibiting superconductivity at temperatures as high as 200 K have spurred an intense search for room-temperature superconductors in hydride materials. Recently, compressed phosphine was reported to metallize at pressures above 45 GPa, reaching a superconducting transition temperature (T_C) of 100 K at 200 GPa. However, neither the exact composition nor the crystal structure of the superconducting phase have been conclusively determined. In this work, the phase diagram of PH_n ($n = 1, 2, 3, 4, 5, 6$) was extensively explored by means of *ab initio* crystal structure predictions using the minima hopping method (MHM). The results do not support the existence of thermodynamically stable PH_n compounds, which exhibit a tendency for elemental decomposition at high pressure even when vibrational contributions to the free energies are taken into account. Although the lowest energy phases of $\text{PH}_{1,2,3}$ display T_C 's comparable to experiments, it remains uncertain if the measured values of T_C can be fully attributed to a phase-pure compound of PH_n .

DOI: 10.1103/PhysRevB.93.020508

In December 2014, Drozdov *et al.* reported a superconducting critical temperature (T_C) of 203 K in an ultradense phase of sulfur hydride (SH_3) [1], identified by *ab initio* crystal structure searches [2], breaking the record- T_C previously held by the cuprates. Subsequent experimental and theoretical studies have confirmed that superconductivity is of conventional nature and occurs in the predicted bcc phase [1,3], demonstrating the potential of *ab initio* crystal structure search methods to identify new superconductors. Several studies have meanwhile appeared in literature, discussing different aspects underlying the exceptional T_C , such as the role of bonding, Coulomb screening, phonon anharmonicity, etc. [4–11].

High- T_C superconductivity based on a conventional electron-phonon (*ep*) coupling mechanism has been suggested by Ashcroft almost fifty years ago. He originally proposed that this could be achieved if hydrogen was sufficiently compressed, a prediction that has not yet been verified due to the required extreme pressures [12–17]. More recently, he suggested that the chemical precompression of hydrogen in hydrogen-rich compounds could be an effective route to reach metallization and high- T_C superconductivity at experimentally accessible pressures [18], stimulating an intense activity of *ab initio* searches and predictions for high- T_C superconducting hydrides [2,19–31]. Until 2014, however, all high-pressure phases which have been synthesized experimentally exhibited rather low T_C [32–35].

Eventually, the discovery of SH_3 showed that high- T_C in hydrogen-rich solids can indeed be achieved. Thus, all stable hydrogen-containing molecules which can be placed into the compressing chamber of a diamond anvil cell are potential candidates for high- T_C superconductors, as long as they remain stable against decomposition, amorphization, and the possible

formation of metal hydrides during the measurement of T_C [32–35].

In fact, less than one year after the discovery of superconductivity in SH_3 , Drozdov *et al.* have very recently reported high- T_C superconductivity in a second hydrogen-rich compound at extreme pressures: resistivity measurements on phosphine (PH_3) show that the samples, which are semiconducting at ambient pressure, metallize above 40 GPa and become superconducting at around 80 GPa, exhibiting a maximum T_C of 100 K at about 200 GPa [36]. Neither the exact composition of the superconducting phase and its crystal structure, nor the mechanism responsible for the high- T_C have been conclusively determined at this point. Analogies with superconducting SH_3 , which was obtained from SH_2 precursor, suggest that the superconductivity in the P-H system is of conventional nature, but that the composition of the superconducting phase might be different from the original PH_3 stoichiometry.

To shed light on this matter we used *ab initio* techniques to map out the high-pressure phase diagram of the P-H binary system by exploring the compositional and configurational space of PH_n with a sophisticated structure prediction method, and estimated the superconducting properties of the most promising phases. We found that all high-pressure binary phases of P and H are metastable with respect to elemental decomposition in the pressure range 100–300 GPa. However, the critical temperatures of the three phases closest to the convex hull (PH , PH_2 , and PH_3) reproduce to a good approximation the experimental T_C values. Possible ways to reconcile our results with experiments are discussed at the end of this manuscript.

To sample the enthalpy landscape, we employed the minima hopping method (MHM) [38,39], which has been successfully

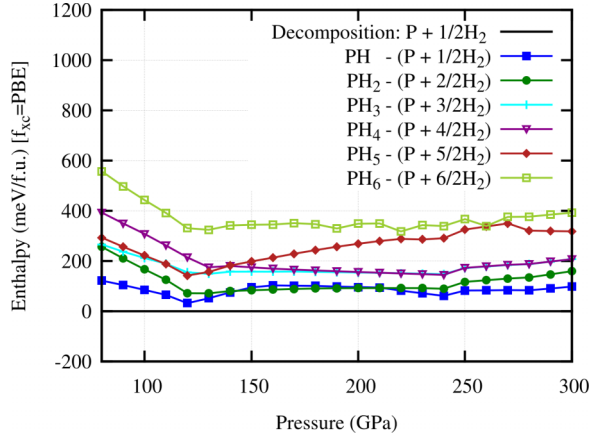


FIG. 1. Calculated enthalpies for PH_n ($n = 1, 2, 3, 4, 5, 6$) for the low-lying structures found in this work. Values are given with respect to the elemental decomposition ($\text{P} + 1/2\text{H}_2$). The reference structures for hydrogen are $P6_3/m$ (0–120 GPa) and $C2/c$ (120–300 GPa) from Ref. [37]. The reference phases for phosphorus are $Pm\bar{3}m$ (0–10 GPa), $R3m$ (20–110 GPa), $P6mm$ (120–240 GPa), $Im\bar{3}m$ (250–270 GPa), and $I43d$ (280–300 GPa). The change in slope at around 120 GPa is due to the phase transition in elemental hydrogen.

used for global geometry optimization¹ in a large variety of applications [40–42], including superconducting materials at high pressure [6,31]. The enthalpies as a function of pressure for the ground-state structures² at each composition are shown in Fig. 1 with respect to elemental decomposition. The ground-state structures were determined by the MHM at 100, 150, 200, and 300 GPa, and further relaxed at intermediate pressures to obtain a smooth phase diagram. An additional search was carried out at zero pressure. The various phases of

¹The MHM was designed to thoroughly scan the low-lying enthalpy landscape of any compound and identify stable phases by performing consecutive short molecular dynamics escape steps followed by local geometry relaxations. The enthalpy surface is mapped out efficiently by aligning the initial molecular dynamics velocities approximately along soft mode directions [66,67], thus exploiting the Bell-Evans-Polanyi [68] principle to steer the search towards low energy structures.

²We explored phases with 1, 2, 3, and 4 formula units of PH_n for stoichiometries $n = 1, 2, 3, 4, 5, 6$ at selected pressures in the range 100–300 GPa. The relaxations to local minima were performed by the fast inertia relaxation engine [69] by taking into account both atomic and cell degrees of freedom. Energy, atomic forces, and stresses were evaluated at the density functional theory (DFT) level with the Perdew-Burke-Erzerhof (PBE) [70] parametrization to the exchange-correlation functional. A plane-wave basis set with a high cutoff energy of 1000 eV was used to expand the wave function together with the projector augmented wave (PAW) method as implemented in the Vienna *ab initio* simulation package VASP [71]. Very dense k meshes were set for the different compositions, at 120 GPa the grids were PH: $20 \times 20 \times 20$, PH_2 : $20 \times 20 \times 16$, PH_3 : $12 \times 12 \times 12$, PH_4 : $14 \times 12 \times 10$, PH_5 : $12 \times 12 \times 8$, PH_6 : $10 \times 14 \times 20$, and for the polymeric phases of PH_2 (6 f.u.): $8 \times 4 \times 12$. Geometry relaxations were performed with tight convergence criteria such that the forces on the atoms were less than 2 meV/Å and the stresses were less than 0.1 meV/Å³.

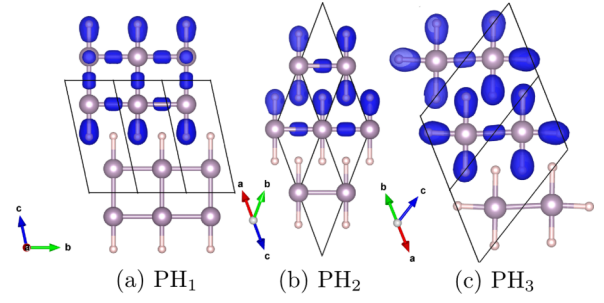


FIG. 2. Low-lying enthalpy structures found for different compositions under pressure at 120 GPa. The large and small spheres denote the P and H atoms, respectively. The ELF at a fixed value of 0.8 is shown in the upper part of each structure.

pure H and P for the convex hull construction were obtained from a structural search, and for hydrogen they coincide with the ones reported by Needs *et al.* [37]: $P6_3/m$ (0–120 GPa) and $C2/c$ (120–300 GPa). The complex phase diagram of elemental phosphorus [43,45], with at least six structural transition between 0 and 300 GPa, is closely reproduced by our calculations, see Ref. [44]. At zero pressure, molecular phosphine (PH_3), as well as the crystalline phases of PH, PH_2 , and PH_3 identified by our MHM runs, are all stable with respect to elemental decomposition (see Ref. [44]). Moreover, we found two compositions (PH and PH_3) forming the convex hull with enthalpies of formation between -50 and -60 meV/atom. In the crystalline phases, the molecules retain their geometry and are held together by van der Waals interactions; these molecular crystals are semiconducting with gaps of 0.9 (PH), 2.1 (PH_2), and 3.7 eV (PH_3), respectively. Given the complexity of the phase diagram of elemental phosphorus, it is likely that the binary phases considered here will undergo several phase transitions between ambient pressure and 100 GPa, but analyzing these transitions is well beyond the scope of this work. Assuming that the PH_3 zero-pressure structure is representative at higher pressures, we estimate a metallization pressure of ~ 35 GPa, which is in accordance with experiments, see Ref. [44] for details.

In the following, we will focus on high pressures (80–200 GPa), which are relevant for superconductivity. The formation enthalpies of all the identified structures are positive and in a range of 30–200 meV/f.u. for hydrides with low hydrogen contents (PH, PH_2 , and PH_3), and larger for higher H content up to PH_6 .

The ground-state structures at 120 GPa of pressure for PH ($I4/mmm$), PH_2 ($I4/mmm$), and PH_3 ($C2/m$) are shown in Fig. 2. The bond lengths are ~ 1.4 Å for the P-H bonds and ~ 2.1 Å for the P-P bonds in all three structures. Figure 2 clearly shows the dominating tendency of P atoms to form polymers with hydrogen saturating the dangling bonds, resulting in 1D chains or 2D layers. This picture is confirmed when looking at the isosurfaces of the electron localization function (ELF), clearly showing that electrons are localized to form P-P and P-H bonds. No or only weak interactions are observed between the polymeric chains, which is in strong contrast to other hydrogen-rich materials that are stable against decomposition and exhibit a 3D network of strongly interacting host atoms and hydrogen [31,46]. With increasing hydrogen content, the dimensionality of the polymers decreases from layers and

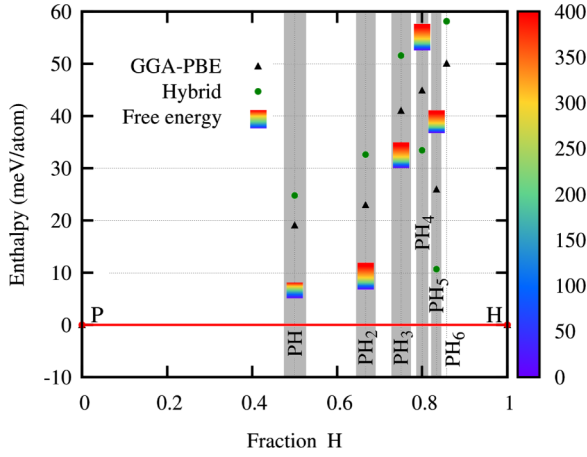


FIG. 3. Predicted formation enthalpies of PH_n with respect to decomposition into P and H at 120 GPa. The solid red line denotes the convex hull of stability. Black triangles show PBE and green squares hybrid functional values (HSE06). The color-gradient scale indicate the free-energy within the harmonic approximation at temperatures up to 400 K (color bar in Kelvin on the right) as computed on top of PBE energies.

sheets (PH, PH_2) to chains (PH_3 , PH_4), until oversaturation is reached and H_2 molecules precipitate, intercalating the P-H polymers in PH_5 and PH_6 .

Figure 1 shows that, although none of the binary phases are thermodynamically stable, some lie very close to the convex hull at around 120 GPa. Therefore an in-depth investigation was conducted to assess whether effects going beyond those included in our MHM searches could stabilize any of these phases in the range between 100 and 150 GPa.

A detailed analysis of the phase stability at 120 GPa is shown in Fig. 3. We first investigated how the use of different exchange-correlation functionals influences the stability of the various compounds. PBE values are shown as black triangles in Fig. 3. In the local density approximation (not shown) we obtain fairly similar phase stabilities. We also report results obtained by means of the more demanding Heyd-Scuseria-Ernzerhof (HSE) hybrid functional [47–50]. Although hybrids are considered to give better results than semilocal functionals for structural and electronic properties in semiconductors [48] and intermetallic alloys [51], they have not been systematically validated for metallic systems, where severe anomalies in the lattice stability and electronic properties have been recently reported [52]. The HSE results, plotted as green squares in Fig. 3, show nevertheless a similar trend as obtained with PBE and LDA. HSE predicts slightly higher formation enthalpies than PBE for PH, PH_2 , PH_3 , and PH_6 , and lower values for PH_4 and PH_5 . Finally, the semiempirical DFT-D2 method of Grimme [53], which takes into account van der Waals interactions, consistently predicted a lower stability of the binary phases compared to PBE. The positive formation enthalpies predicted by all four exchange-correlation functionals strongly suggest that none of the binary PH_n phases are in fact thermodynamically stable.

Next, we investigated the influence of vibrational entropy and zero-point energy (ZPE) on the phase stability. Phonon calculations were carried out with the frozen phonon approach as implemented in the PHONOPY package [54] with sufficiently

large supercells. The ZPE and free energy within the harmonic approximation at temperatures between 0 and 400 K shown as colored gradients in Fig. 3. There is a clear distinction in the vibrational effect on the stability for PH_n phases with high and low hydrogen content: PH, PH_2 , and PH_3 increase in stability, whereas PH_4 and PH_5 decrease. This behavior can be attributed to the existence of H_2 molecules in the crystal lattice of the hydrogen-rich phases, which induce high-energy vibrational modes responsible for an increased ZPE.

For PH, the formation energy is less than 5 meV/atom at 0 K, whereas for PH_2 and PH_3 , it is about 7 and 30 meV/atom, respectively. Comparing the free energies at finite temperatures reveals that all phases are destabilized by vibrational entropy by a few meV, pushing them away from the convex hull with increasing temperature. Since anharmonic effects become increasingly important at higher temperatures, we recomputed the free energy for PH, PH_2 , and PH_3 within the quasiharmonic approximation, taking into account the thermal lattice expansion. These calculations, however, showed only minor effects on the stabilities and the distance from the convex hull of all three binary phases slightly increased by a few meV per atom.

Having ruled out that any of the standard corrections to the electronic enthalpy can stabilize our phases in the experimentally relevant regime, we are left with the question of which phase and chemical composition was experimentally observed by Drozdov *et al.* We can rule out that the superconductivity observed is due to some residual elemental phase, as hydrogen is not metallic at these pressures and elemental phosphorus displays much lower critical temperatures [55], not higher than a few Kelvin.

On the other hand, our phonon calculations show that the ground states at fixed compositions of PH_1 , PH_2 , and PH_3 are all dynamically stable, i.e., with no imaginary modes in the whole Brillouin zone. Therefore one of these metastable phases might have been synthesized through a nonequilibrium process or possibly through anisotropic stress in the anvil cell, as the order of magnitude of the relevant energy barriers in these cases could be in the range of few tens of meV. In fact, the compositions closest to the hull are PH and PH_2 , indicating a possible decomposition of the original phosphine molecules (PH_3) under pressure into PH and PH_2 , similarly to what is observed in sulfur hydrides where the initial, molecular SH_2 decomposes under pressure to form SH_3 .

To assess whether any of these three metastable phases could be a reasonable candidate for superconductivity, we calculated the Eliashberg spectral functions for the electron-phonon (*ep*) interaction:

$$\alpha^2 F(\omega) = \frac{1}{N_{E_F}} \sum_{\mathbf{k}, \mathbf{q}, \nu} |g_{\mathbf{k}, \mathbf{k}+\mathbf{q}, \nu}|^2 \delta(\epsilon_{\mathbf{k}}) \delta(\epsilon_{\mathbf{k}+\mathbf{q}}) \delta(\omega - \omega_{\mathbf{q}, \nu}), \quad (1)$$

where N_{E_F} is the DOS at the Fermi level, $\omega_{\mathbf{q}, \nu}$ is the phonon frequency of mode ν at wave vector \mathbf{q} and $|g_{\mathbf{k}, \mathbf{k}+\mathbf{q}, \nu}|$ is the electron-phonon matrix element between two electronic states with momenta \mathbf{k} and $\mathbf{k} + \mathbf{q}$ at the Fermi level.

From the Eliashberg function, we also obtained the electron-phonon coupling constant λ and the logarithmic average phonon frequency ω_{ln} [56,57] (which, in the McMillan-Allen-Dynes parametrization for T_C , sets the energy scale for

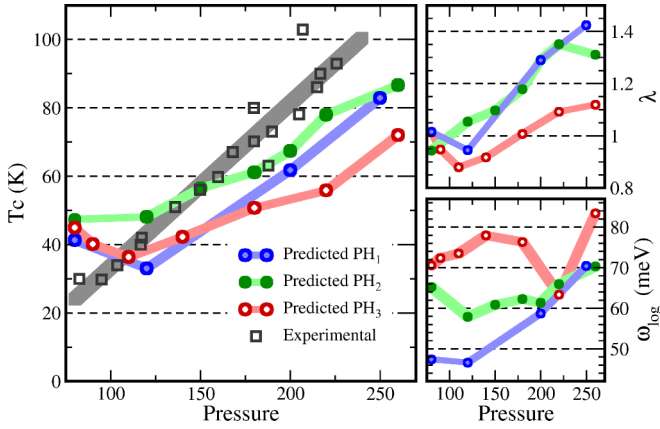


FIG. 4. (Left) SCDFT calculated critical temperatures T_C for PH (blue), PH_2 (green), and PH_3 (red) as a function of pressure. Experimental T_C by resistivity measurements from Drozdov *et al.* [36] are shown in black squares. Overall a good agreement is found between the experimental values and those for PH, PH_2 , and PH_3 . Although the PH_2 composition shows significantly better agreement. (Right) Trend in pressure of the (BCS-like) electron phonon coupling coefficient λ (top panel) and of the phononic characteristic frequency ω_{ln} (bottom panel) as a function of pressure.

the phononic pairing). In order to avoid using the empirical μ^* parameter and bias the theoretical predictions towards the experiments, we computed the critical temperatures within density functional theory for superconductors (SCDFT), which uses as input the Eliashberg function in an isotropic approximation, while the residual Coulomb forces in the Cooper pairing are included within the static random phase approximation [58–61], as used in Refs. [6,62].

The values of T_C are shown in Fig. 4 and are compared to the experimental values reported by Drozdov *et al.* [36]. In the two right panels of the same figure, we show λ and ω_{ln} for the three phases as a function of pressure.³

Our calculated behavior of T_C with respect to pressure shows a fair agreement with experiments for all three structures (PH, PH_2 , and PH_3); the best agreement is found for PH_2 , which has a T_C of 40 K at 100 GPa that increases under pressure and reaches a maximum value of 78 K at 220 GPa. The PH system shows the best agreement in the rate at which T_C grows with pressure in the 120–260 GPa window ($dT_C/dP \simeq 0.4$ K/GPa), while showing a high pressure shift of about 20 GPa with respect to the experimental data.

The similar superconducting behavior of the three compounds results from the compensation of different behaviors

³Electronic bands, vibrational frequencies, and electron-phonon matrix elements were computed within density functional perturbation theory [72–74], as implemented in the QUANTUM ESPRESSO and ABINIT code. We employed norm-conserving pseudopotentials for H and P, with a plane-wave cutoff of 80 Ry; phonon frequencies and electron-phonon were computed on coarse (8^3 , 6^3 , and 4^3 k points for PH, PH_2 , and PH_3 , respectively), and interpolated on denser grids using force constants; for the electronic integration, we employed Monkhorst-Pack grids of 8^3 k points for the self-consistent calculations; much denser (up to 30^3 points) grids were used for Fermi-surface integrations.

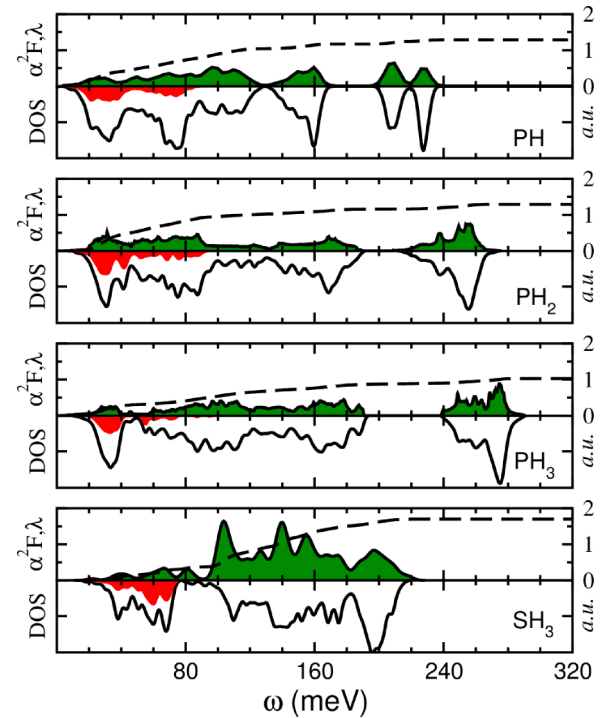


FIG. 5. Eliashberg spectral function (solid line) and frequency-dependent ep coupling parameters $\lambda(\omega)$ (dashed line)—top panels—and phonon density of states (DOS)—bottom panels—for the three PH_n compounds considered in the present study and SH_3 at 200 GPa. The shaded area (red) in the DOS panels is the P/S partial phonon DOS.

of λ and ω_{ln} , shown in the right panels of the same figure. These reflect different features of the three Eliashberg functions, shown in Fig. 5, together with that of SH_3 for reference. The $PH_{1,2,3}$ spectra have an overall similar shape, i.e., they are roughly proportional to the phonon density of states, dominated by P modes at low frequencies (<80 meV), and hydrogen modes at high frequencies.

A gap separates the hydrogen bond-bending vibrations from the rest of the spectrum; this part moves to higher energies with increasing hydrogen content, but has very little influence on T_C due to the high frequencies involved. The spectrum of SH_3 is more compact, extending up to 200 meV, with higher peaks in $\alpha^2F(\omega)$, thus resulting in a large value of $\lambda(\simeq 1.9)$.

As more and more theoretical predictions of new superconducting hydrides are available, there is an increasing effort towards a systematic understanding of the factors leading to high T_C [26,46]. It is becoming clear that the original idea of Ashcroft [18], that the heavier atoms merely exert chemical pressure on the hydrogen lattice, is oversimplified, and other factors, such as the formation of strong atomic bonds between H and the heavier elements, play a crucial role. A good indicator for the tendency of a material to follow one or another behavior is the electronegativity of the heavy atom. Atoms which are less electronegative than H tend to form solids which contain H_2 units with large characteristic vibration frequencies, but relatively weak matrix elements (electron-phonon coupling). More electronegative atoms, on the other hand, tend to form polar-covalent bonds, which couple strongly to phonons [9,46].

Phosphorus, with an electronegativity equal to that of hydrogen, lies on the border between the two regions and for the three hydrides considered in this study the electronic structure indicates a strong P-H hybridization in the whole energy range (see Ref. [44]). The values of the electronic density of state (DOS) at the Fermi level— N_{E_F} —are comparable (0.31–0.38 st/eVf.u.), and sensibly lower than those in SH_3 (0.54). The ratio $\eta = \lambda/N_{E_F}$, which can give an indication of the “stiffness” of the underlying lattice, ranges from 3 in PH_3 to 3.8 in PH , and is 3.6 in SH_3 .

In practice, $\text{PH}_{1,2,3}$ and SH_3 have a quite similar bonding and lattice stiffness to each other: what makes the latter exhibit a yet unmatched record T_C is the extremely high value of its N_{E_F} , due to the presence of the van Hove singularity close to the Fermi level [10,11]. As the Fermi level of PH_2 and PH_3 falls in a shallow minimum of the density of states (see Ref. [44]), the same effect could be used to increase their T_C , by doping a small fraction of S or Si impurities into the samples.

In conclusion, the phase stability and superconducting properties of the recently reported PH_3 compound under pressure have been investigated with *ab initio* calculations. Our extensive structural searches show that the hydrogen-rich phosphorus phases are thermodynamically unstable in the high-pressure regime of the phase diagram. Although including vibrational zero-point effects in our calculations improves the stability of PH , PH_2 , and PH_3 , they remain metastable. Nevertheless, in view of their small distance from the convex hull, any of these structures may have been synthesized through nonequilibrium or by anharmonic effects, as discussed in Refs. [5,63]. Several of them were predicted to be good phonon-mediated superconductors and could thus in principle account for the measured high- T_C in experiments. In our opinion, the phase/composition that yields the best agreement with experiments are PH and PH_2 , which are both close to the convex hull (<7 meV/atom) and would show a pressure

dependence in T_C similar to the experimental measurements. It is still unclear if the experimentally observed high- T_C can be fully attributed to a phase of a binary phosphorus hydride, and further experiments are called for to validate both our predictions and the results reported by Drozdov *et al.* [36]. Finally, our calculations give a strong indication that the observed critical temperatures are those to be expected for the low energy, low-H content phases of the P-H system.

Note added. While writing the present manuscript, we became aware of two works, which report structural searches of phosphorus hydrides, employing evolutionary algorithms [64,65]. Both studies agree with our conclusions that none of the predicted phases are thermodynamically stable in the pressure range of 100–200 GPa. Shamp *et al.* [64] also suggest an $I4/mmm$ PH_2 structure as a possible candidate for the high- T_C phase. They also report a *polymeric* PH_2 structure, which is more stable at low pressures. Based on our calculations, however, the *polymeric* structures for PH_2 show higher enthalpies than the $I4/mmm$ structure.

J.A.F.-L. acknowledges the EU’s 7th Framework Marie-Curie Program within the “ExMaMa” Project (329386). M.A. gratefully acknowledges support from the Novartis Universität Basel Excellence Scholarship for Life Sciences and the Swiss National Science Foundation. C.H. and L.B. acknowledge funding from the FWF-SFB ViCoM F41 P15 and computational resources from the dCluster of the Graz University of Technology and the VSC3 of the Vienna University of Technology. C.W. acknowledges financial support from the U.S. Department of Energy under Grant DE-FG02-07ER46433. Computational resources from the Swiss National Supercomputing Center (CSCS) in Lugano (Project s499) and the National Energy Research Scientific Computing Center, which is supported by the Office of Science of the U.S. Department of Energy under Contract No. DE-AC02-05CH11231, are acknowledged. This work was done within the NCCR MARVEL project.

- [1] A. P. Drozdov, M. I. Erements, I. A. Troyan, V. Ksenofontov, and S. I. Shylin, *Nature (London)* **525**, 73 (2015).
- [2] D. Duan, Y. Liu, F. Tian, D. Li, X. Huang, Z. Zhao, H. Yu, B. Liu, W. Tian, and T. Cui, *Sci. Rep.* **4** (2014).
- [3] M. Einaga, M. Sakata, T. Ishikawa, K. Shimizu, M. Erements, A. Drozdov, I. Troyan, N. Hirao, and Y. Ohishi, *arXiv:1509.03156*.
- [4] N. Bernstein, C. S. Hellberg, M. D. Johannes, I. I. Mazin, and M. J. Mehl, *Phys. Rev. B* **91**, 060511 (2015).
- [5] I. Errea, M. Calandra, C. J. Pickard, J. Nelson, R. J. Needs, Y. Li, H. Liu, Y. Zhang, Y. Ma, and F. Mauri, *Phys. Rev. Lett.* **114**, 157004 (2015).
- [6] J. A. Flores-Livas, A. Sanna, and E. K. U. Gross, *arXiv:1501.06336* [cond-mat.supr-con].
- [7] D. Duan, X. Huang, F. Tian, D. Li, H. Yu, Y. Liu, Y. Ma, B. Liu, and T. Cui, *Phys. Rev. B* **91**, 180502 (2015).
- [8] R. Akashi, M. Kawamura, S. Tsuneyuki, Y. Nomura, and R. Arita, *Phys. Rev. B* **91**, 224513 (2015).
- [9] C. Heil and L. Boeri, *Phys. Rev. B* **92**, 060508 (2015).
- [10] Y. Quan and W. E. Pickett, *arXiv:1508.04491*.
- [11] L. Ortenzi, E. Cappelluti, and L. Pietronero, *arXiv:1511.04304* [cond-mat.mtrl-sci].
- [12] N. Ashcroft, *Phys. Rev. Lett.* **21**, 1748 (1968).
- [13] P. Cudazzo, G. Profeta, A. Sanna, A. Floris, A. Continenza, S. Massidda, and E. K. U. Gross, *Phys. Rev. Lett.* **100**, 257001 (2008).
- [14] P. Cudazzo, G. Profeta, A. Sanna, A. Floris, A. Continenza, S. Massidda, and E. K. U. Gross, *Phys. Rev. B* **81**, 134505 (2010).
- [15] P. Cudazzo, G. Profeta, A. Sanna, A. Floris, A. Continenza, S. Massidda, and E. K. U. Gross, *Phys. Rev. B* **81**, 134506 (2010).
- [16] R. Szczechśniak and M. Jarosik, *Solid State Commun.* **149**, 2053 (2009).
- [17] J. M. McMahon and D. M. Ceperley, *Phys. Rev. B* **84**, 144515 (2011).
- [18] N. W. Ashcroft, *Phys. Rev. Lett.* **92**, 187002 (2004).
- [19] J. S. Tse, Y. Yao, and K. Tanaka, *Phys. Rev. Lett.* **98**, 117004 (2007).
- [20] X.-J. Chen, V. V. Struzhkin, Y. Song, A. F. Goncharov, M. Ahart, Z. Liu, H.-k. Mao, and R. J. Hemley, *Proc. Natl. Acad. Sci. USA* **105**, 20 (2008).
- [21] D. Y. Kim, R. H. Scheicher, S. Lebègue, J. Prasongkit, B. Arnaud, M. Alouani, and R. Ahuja, *Proc. Natl. Acad. Sci. USA* **105**, 16454 (2008).

- [22] J. Feng, R. G. Hennig, N. W. Ashcroft, and R. Hoffmann, *Nature (London)* **451**, 445 (2008).
- [23] S. Wang, H.-k. Mao, X.-J. Chen, and W. L. Mao, *Proc. Natl. Acad. Sci. USA* **106**, 14763 (2009).
- [24] Y. Yao and D. D. Klug, *Proc. Natl. Acad. Sci. USA* **107**, 20893 (2010).
- [25] G. Gao, A. R. Oganov, P. Li, Z. Li, H. Wang, T. Cui, Y. Ma, A. Bergara, A. O. Lyakhov, T. Itaka, and G. Zou, *Proc. Natl. Acad. Sci. USA* **107**, 1317 (2010).
- [26] D. Y. Kim, R. H. Scheicher, H.-k. Mao, T. W. Kang, and R. Ahuja, *Proc. Natl. Acad. Sci. USA* **107**, 2793 (2010).
- [27] Y. Li, G. Gao, Y. Xie, Y. Ma, T. Cui, and G. Zou, *Proc. Natl. Acad. Sci. USA* **107**, 15708 (2010).
- [28] D. Zhou, X. Jin, X. Meng, G. Bao, Y. Ma, B. Liu, and T. Cui, *Phys. Rev. B* **86**, 014118 (2012).
- [29] J. Hooper, T. Terpstra, A. Shamp, and E. Zurek, *J. Phys. Chem. C* **118**, 6433 (2014).
- [30] T. Muramatsu, W. K. Wanene, M. Somayazulu, E. Vinitzky, D. Chandra, T. A. Strobel, V. V. Struzhkin, and R. J. Hemley, *J. Phys. Chem. C* **119**, 18007 (2015).
- [31] J. A. Flores-Livas, M. Amsler, T. J. Lenosky, L. Lehtovaara, S. Botti, M. A. L. Marques, and S. Goedecker, *Phys. Rev. Lett.* **108**, 117004 (2012).
- [32] M. I. Eremets, I. A. Trojan, S. A. Medvedev, J. S. Tse, and Y. Yao, *Science* **319**, 1506 (2008).
- [33] O. Degtyareva, J. E. Proctor, C. L. Guillaume, E. Gregoryanz, and M. Hanfland, *Solid State Commun.* **149**, 1583 (2009).
- [34] M. Hanfland, J. E. Proctor, C. L. Guillaume, O. Degtyareva, and E. Gregoryanz, *Phys. Rev. Lett.* **106**, 095503 (2011).
- [35] D. Y. Kim, R. H. Scheicher, C. J. Pickard, R. J. Needs, and R. Ahuja, *Phys. Rev. Lett.* **107**, 117002 (2011).
- [36] A. Drozdov, M. I. Eremets, and I. A. Trojan, [arXiv:1508.06224](https://arxiv.org/abs/1508.06224) [cond-mat.supr-con].
- [37] C. J. Pickard and R. J. Needs, *Nat. Phys.* **3**, 473 (2007).
- [38] S. Goedecker, *J. Chem. Phys.* **120**, 9911 (2004).
- [39] M. Amsler and S. Goedecker, *J. Chem. Phys.* **133**, 224104 (2010).
- [40] M. Amsler, J. A. Flores-Livas, L. Lehtovaara, F. Balima, S. A. Ghasemi, D. Machon, S. Pailhès, A. Willand, D. Caliste, S. Botti, A. San Miguel, S. Goedecker, and M. A. L. Marques, *Phys. Rev. Lett.* **108**, 065501 (2012).
- [41] M. Amsler, J. A. Flores-Livas, T. D. Huan, S. Botti, M. A. L. Marques, and S. Goedecker, *Phys. Rev. Lett.* **108**, 205505 (2012).
- [42] S. Botti, J. A. Flores-Livas, M. Amsler, S. Goedecker, and M. A. L. Marques, *Phys. Rev. B* **86**, 121204 (2012).
- [43] T. Sugimoto, Y. Akahama, H. Fujihisa, Y. Ozawa, H. Fukui, N. Hirao, and Y. Ohishi, *Phys. Rev. B* **86**, 024109 (2012).
- [44] See Supplemental Material at <http://link.aps.org/supplemental/10.1103/PhysRevB.93.020508> for the predicted phase diagram of elemental phosphorus; the electronic band structure and density of states for the ground states of PH₁, PH₂, and PH₃; the phase diagram of P_xH_{1-x} at ambient pressure; the metalization behavior of PH₃; and the enthalpies of the polymeric phase of PH₂ as a function of pressure.
- [45] M. Marqués, G. J. Ackland, L. F. Lundegaard, S. Falconi, C. Hejny, M. I. McMahon, J. Contreras-García, and M. Hanfland, *Phys. Rev. B* **78**, 054120 (2008).
- [46] S. Zhang, Y. Wang, J. Zhang, H. Liu, X. Zhong, H.-F. Song, G. Yang, L. Zhang, and Y. Ma, [arXiv:1502.02607](https://arxiv.org/abs/1502.02607).
- [47] J. Paier, M. Marsman, K. Hummer, G. Kresse, I. C. Gerber, and J. G. Ángyán, *J. Chem. Phys.* **124**, 154709 (2006).
- [48] J. Heyd, J. E. Peralta, G. E. Scuseria, and R. L. Martin, *J. Chem. Phys.* **123**, 174101 (2005).
- [49] J. Heyd, G. E. Scuseria, and M. Ernzerhof, *J. Chem. Phys.* **124**, 219906 (2006).
- [50] J. Paier, M. Marsman, K. Hummer, G. Kresse, I. C. Gerber, and J. G. Ángyán, *J. Chem. Phys.* **125**, 249901 (2006).
- [51] Y. Zhang, G. Kresse, and C. Wolverton, *Phys. Rev. Lett.* **112**, 075502 (2014).
- [52] W. Gao, T. A. Abtew, T. Cai, Y. Y. Sun, S. B. Zhang, and P. Zhang, [arXiv:1504.06259](https://arxiv.org/abs/1504.06259) [cond-mat.mtrl-sci].
- [53] S. Grimme, *J. Computat. Chem.* **27**, 1787 (2006).
- [54] A. Togo, F. Oba, and I. Tanaka, *Phys. Rev. B* **78**, 134106 (2008).
- [55] M. Karuzawa, M. Ishizuka, and S. Endo, *J. Phys.: Condens. Matter* **14**, 10759 (2002).
- [56] J. P. Carbotte, *Rev. Mod. Phys.* **62**, 1027 (1990).
- [57] P. B. Allen and B. Mitrović, in *Theory of Superconducting Tc*, Solid State Physics Vol. 37 (Academic Press, London, 1983), pp. 1–92.
- [58] L. N. Oliveira, E. K. U. Gross, and W. Kohn, *Phys. Rev. Lett.* **60**, 2430 (1988).
- [59] M. Lüders, M. A. L. Marques, N. N. Lathiotakis, A. Floris, G. Profeta, L. Fast, A. Continenza, S. Massidda, and E. K. U. Gross, *Phys. Rev. B* **72**, 024545 (2005).
- [60] M. A. L. Marques, M. Lüders, N. N. Lathiotakis, G. Profeta, A. Floris, L. Fast, A. Continenza, E. K. U. Gross, and S. Massidda, *Phys. Rev. B* **72**, 024546 (2005).
- [61] S. Massidda, F. Bernardini, C. Bersier, A. Continenza, P. Cudazzo, A. Floris, H. Glawe, M. Monni, S. Pittalis, G. Profeta, A. Sanna, S. Sharma, and E. K. U. Gross, *Supercond. Sci. Technol.* **22**, 034006 (2009).
- [62] J. A. Flores-Livas and A. Sanna, *Phys. Rev. B* **91**, 054508 (2015).
- [63] E. A. Engel, B. Monserrat, and R. J. Needs, *Phys. Rev. X* **5**, 021033 (2015).
- [64] A. Shamp, T. Terpstra, T. Bi, Z. Falls, P. Avery, and E. Zurek, [arXiv:1509.05455](https://arxiv.org/abs/1509.05455).
- [65] Y. Fu, X. Du, L. Zhang, F. Peng, M. Zhang, C. J. Pickard, R. J. Needs, D. J. Singh, W. Zheng, and Y. Ma, [arXiv:1510.04415](https://arxiv.org/abs/1510.04415) [cond-mat.mtrl-sci].
- [66] S. Roy, S. Goedecker, M. J. Field, and E. Penev, *J. Phys. Chem. B* **113**, 7315 (2009).
- [67] M. Sicher, S. Mohr, and S. Goedecker, *J. Chem. Phys.* **134**, 044106 (2011).
- [68] F. Jensen, *Introduction to Computational Chemistry*, 2nd ed. (John-Wiley, Amsterdam, 2011).
- [69] E. Bitzek, P. Koskinen, F. Gähler, M. Moseler, and P. Gumbsch, *Phys. Rev. Lett.* **97**, 170201 (2006).
- [70] J. P. Perdew, K. Burke, and M. Ernzerhof, *Phys. Rev. Lett.* **77**, 3865 (1996).
- [71] G. Kresse and J. Furthmüller, *Comput. Mater. Sci.* **6**, 15 (1996).
- [72] S. Baroni, S. de Gironcoli, A. Dal Corso, and P. Giannozzi, *Rev. Mod. Phys.* **73**, 515 (2001).
- [73] X. Gonze and J.-P. Vigneron, *Phys. Rev. B* **39**, 13120 (1989).
- [74] S. Y. Savrasov and D. Y. Savrasov, *Phys. Rev. B* **54**, 16487 (1996).